Warren, R.L., Tassieri, M., Li, X., Glidle, A., Paterson, D.J., Carlsson, A., and Cooper, J.M. (2013) Rheology at the micro-scale: new tools for bio-analysis. In: Optical Methods for Inspection, Characterization and Imaging of Biomaterials, 13-16 May 2013, Munich, Germany.

Copyright © 2013 SPIE

A copy can be downloaded for personal non-commercial research or study, without prior permission or charge

The content must not be changed in any way or reproduced in any format or medium without the formal permission of the copyright holder(s)

When referring to this work, full bibliographic details must be given

http://eprints.gla.ac.uk/80448/

Deposited on: 31 May 2013

Enlighten – Research publications by members of the University of Glasgow
http://eprints.gla.ac.uk

Invited Paper

Rheology at the micro-scale: new tools for bio-analysis

Rebecca L. Warren, Manlio Tassieri, Xiang Li, Andrew Glidle, David J. Paterson, Allan Carlsson, and Jonathan M. Cooper

Division of Biomedical Engineering, School of Engineering, University of Glasgow, Glasgow G12 8LT, UK

ABSTRACT

We present a simple and *non-invasive* experimental procedure to measure the linear viscoelastic properties of cells by passive particle tracking microrheology. In order to do this, a generalised Langevin equation is adopted to relate the time-dependent thermal fluctuations of a probe sensor, immobilised to the cell's membrane, to the frequency-dependent viscoelastic moduli of the cell. The method has been validated by measuring the linear viscoelastic response of a soft solid and then applied to cell physiology studies. It is shown that the viscoelastic moduli are related to the cell's cytoskeletal structure, which in this work is modulated either by inhibiting the actin/myosin-II interactions by means of blebbistatin *or* by varying the solution osmolarity from iso- to hypo-osmotic conditions. The insights gained from this form of rheological analysis promises to be a valuable addition to physiological studies; e.g. cell physiology during pathology and pharmacological response.

Keywords: Microrheology, Cell Physiology, Cell Mechanics.

1. INTRODUCTION

The study of physical and biological phenomena at very small scales has been made possible thanks to developments in micro- and nano-scale science, coupled with the commercialisation of new instrumentation and equipment, available at relatively low prices. These trends have also been seen in Lab-on-a-Chip [1], where the rapid analysis of complex biological solutions has enabled new technologies in medical diagnostics and drug delivery. Sitting between the two areas of instrumentation and microfluidics is the field of rheology, which is the study of materials viscoelastic properties, exploring the interactions between macromolecules and their solvents. Microrheology is a branch of rheology, which is underpinned by the same principles as conventional bulk rheology although experiments and information are obtained on micron length scales. The development of techniques in microrheology has dramatically reduced the sample volume that can be analysed (down to $\sim 1\mu l$) compared with the sample volume used for conventional rheology (more than $1ml$); making it particularly suitable for use with rare and expensive materials, including biological samples [2,3]. As a consequence of these small scales, microrheology measurements have the potential to be performed *in situ* in an environment that can not be reached by bulk experiments; e.g. inside a living cell [4].

The mechanical properties of a cell's cytoskeleton can influence factors such as growth, apoptosis, motility, signal transduction and gene expression [5]. Related to this, there is a desire to be able to provide a rheological interpretation of the cell's viscoelastic properties that has the potential to yield quantitative information on the cell's cytoskeletal structure and dynamics [6–11]. Consequently, in this work, we have developed a means of using passive particle tracking microrheology measurements to quantitatively measure changes in the viscoelastic properties of a cell as a consequence (in this case) of simple changes in its external environment, i.e. subjecting a cell either to the addition of blebbistatin to the cell bath *or* to a hypo-osmotic shock.

The interpretation of microrheology measurements performed on living systems such as cells is not trivial and represents a lively point of discussion in literature [6–10]. The debate is centred on the violation of the fluctuation-dissipation theorem (FDT) because of the existence of non-thermal forces, generated by protein-protein interactions (e.g. actin/myosin-II

Further author information: Send correspondence to M.T.
E-mail: Manlio.Tassieri@glasgow.ac.uk

Optical Methods for Inspection, Characterization, and Imaging of Biomaterials, Pietro Ferraro, Monika Ritsch-Marte, Simonetta Grilli, David Stifter, Eds., Proc. of SPIE Vol. 8792, 879214
© 2013 SPIE · CCC code: 0277-786X/13/$18 · doi: 10.1117/12.2025254

Downloaded From: http://proceedings.spiedigitallibrary.org/ on 05/30/2013 Terms of Use: http://spiedl.org/terms

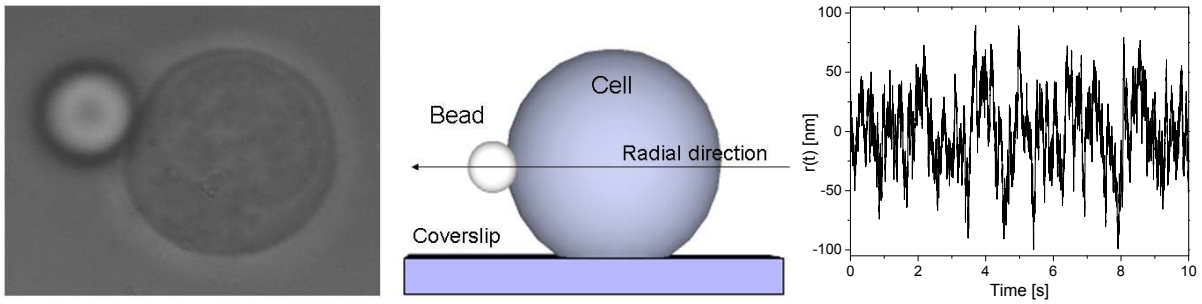

Figure 1. (Left) Top-view of a $5\mu m$ diameter silica bead bound to the surface of a Jurkat cell. (Centre) Schematic side-view of the left image. (Right) The thermal fluctuations of a $5\mu m$ silica bead chemically bound to the surface of a Jurkat cell. Images were analysed in real-time and the coordinates of the bead's centre of mass were stored directly on the random-access memory (RAM) of the computer, at frequency $\simeq 1kHz$, using our own suite of image analysis software written in LabVIEW[21].

interactions), governing the probe motion at relatively low frequencies (i.e. $\lesssim 1Hz$). However, it is important to highlight that, at high frequencies (i.e. $\gtrsim 1Hz$), all the competing theories and the related experimental evidences addressed to resolving the debate agree on the fact that in cells the thermal fluctuations dominate on those fluctuations induced by protein-protein interactions (e.g. motor proteins); i.e. the cytosckeleton can be considered as if it were at thermal equilibrium, thus the applicability of the FDT.

The linear viscoelastic (LVE) properties of a material can be represented by the frequency-dependent dynamic complex modulus $G^*(\omega)$, which provides information on both the viscous and the elastic nature of the material at different frequencies ω; it is defined as the ratio between the Fourier transforms (denoted by the symbol "ˆ") of the applied stress $\sigma(t)$ and the resulting strain $\gamma(t)$[12]:

$$G^*(\omega) = \frac{\hat{\sigma}(t)}{\hat{\gamma}(t)} = G'(\omega) + iG''(\omega) \tag{1}$$

where the real and the imaginary parts of $G^*(\omega)$ are defined as the storage (elastic) $G'(\omega)$ and the loss (viscous) $G''(\omega)$ moduli, respectively; and i is the imaginary unit (i.e. $i^2 = -1$).

In this work we present a straightforward procedure for measuring the *in vivo* linear viscoelastic properties of single cells *via* passive particle tracking microrheology of single beads attached to the cells' exterior. This method has advantages over both complicated active microrheology techniques, where complex experimental set-ups are necessary to exert an external force for performing stress-controlled measurements; and *invasive* passive video particle tracking of submicron-probes embedded (either *via* endocytosis *or* micropipette injection) within the cell's cytoskeleton[13–20].

The procedure consists of measuring the thermal fluctuations of a bead chemically bound to the cell's exterior (Figure 1), for a sufficiently long time. A generalised Langevin equation was adopted to relate the time-dependent bead trajectory, $\vec{r}(t)$, to the frequency-dependent moduli of the cell. Notably, the procedure presented here represents an alternative methodology that can be extended to many experimental formats and provides a simple addition to existing cellular physiology studies; e.g. those monitoring cell pharmacological response. Indeed, when compared to single cell viscoelasticity assays using techniques such as magnetic tweezers, atomic force microscopy and an optical stretcher, as employed in[13–20], our method has the advantage of revealing the changes of the cell's viscoelastic properties over a wide range of frequencies (here from $\sim 1\ Hz$ up to $\sim 1\ kHz$), to a high level of accuracy.

2. METHODOLOGY

2.1 Optical trapping system

Optical trapping is achieved by means of a titanium-sapphire laser with a $5W$ pump (Verdi V5 laser; Coherent Inc.), which provides up to $1W$ at 830 nm. The tweezers are based around an inverted microscope, where the same objective lens (100x, 1.3 numerical aperture, Zeiss, Plan-Neofluor) is used both to focus the trapping beam and to image the thermal fluctuations of $5\mu m$ diameter silica bead. Samples are mounted on a motorised microscope stage (Prior Pro-Scan II). A complementary

Downloaded From: http://proceedings.spiedigitallibrary.org/ on 05/30/2013 Terms of Use: http://spiedl.org/terms

metal-oxide semiconductor camera (Dalsa Genie HM640 GigE) takes high-speed images of a reduced field of view. These images are processed in real-time at $\simeq 1kHz$ using our own LabVIEW (National Instruments) particle tracking software[21] running on a standard personal computer.

2.2 Sample preparation

Two sets of chemically coated $5\mu m$ diameter silica beads were used to carry out different experiments. One set was made by streptavidin-coated silica beads (Bangs Laboratories Inc) and the second set was prepared in our lab by attaching Anti-CD4+ (Invitrogen) to $5\mu m$ carboxylate functionalised silica beads (Bangs Laboratories Inc) by following a protocol already described in literature[22]. The Jurkat cells were obtained from ATCC (clone E6-1, TIB-152) and maintained in RPMI 1640 media containing L-Glutamine and 25mM HEPES [Gibco, Invitrogen]. Prior to the experiment they were suspended in PBS [Gibco, Invitrogen] with an osmolarity of 275-304 mOsm, then mixed with the functionalised beads and allowed to equilibrate for $\sim$10min. Beads were optically trapped and moved to the equatorial plane of the cell, where they were held for a sufficient time ($\sim$2 min) until the binding process was completed.

2.3 Analytical model

The equation describing the *pseudo* Brownian fluctuation of the randomly varying bead position $\vec{r}(t)\forall t$ can be derived by means of a generalised Langevin equation:

$$m\vec{a}(t) = \vec{f}_R(t) - \int_0^t [\zeta_c(t-\tau) + \zeta_s(t-\tau)]\vec{v}(\tau)d\tau \tag{2}$$

where m is the mass of the particle, $\vec{a}(t)$ is its acceleration, $\vec{v}(t)$ is the bead velocity and $\vec{f}_R(t)$ is the usual Gaussian white noise term that models stochastic thermal forces acting on the particle. The integral term represents the total damping force acting on the bead, which, based on the superposition principle, incorporates two generalised time-dependent memory functions $\zeta_c(t)$ and $\zeta_s(t)$ that are representative of the viscoelastic nature of the cell and the solvent, respectively. These memory functions are directly related to the materials' complex modulus as shown hereafter.

In the case of the solvent, which in this work is the culture media surrounding the cell, the relationship between memory function and complex modulus is straightforward. Indeed, to a first approximation, using the assumptions adopted by Mason and Weitz[23] when studying the motion of thermally excited free particles, at thermal equilibrium the complex viscoelastic modulus of the solvent is related to the memory function $\zeta_s(t)$ by the expression: $G_s^*(\omega) = i\omega\hat{\zeta}_s(\omega)/6\pi R$, where R is the bead radius and $\hat{\zeta}_s(\omega)$ is the Fourier transform of $\zeta_s(t)$. In the case of the cell, we assume a similar relationship between $G_c^*(\omega)$ and $\zeta_c(t)$ to that given above for the solvent, but with a different constant of proportionality that we will call β; i.e., $G_c^*(\omega) = i\omega\hat{\zeta}_c(\omega)/\beta$. Note that, β may vary for different cells because it depends on (*i*) the cell radius (R_c), (*ii*) the number of the chemical bonds between the bead and the cell, (*iii*) the contact area between the cell and the glass coverslip, and (*iv*) the relative position of the bead with respect to both the cell's equatorial plane and the glass coverslip. In this study we focus only on the changes in cell dynamics due to either the addition of blebbistatin to the cell bath *or* a hypo-osmotic shock. This can be achieved since all the above experimental parameters, with the exception of R_c for the case of the hypo-osmotic shock, are (in good approximation) time-independent, and will not change significantly during the course of a set of measurements. This is shown in Figure 3 later in the manuscript, for measurements performed on cells in iso-osmotic condition.

In addition, it is important to highlight that in all cases the cells maintain a spherical shape well beyond the duration of the experiments. Moreover, the cells adhered to the coverslip and no drift was observed during the experiments. Finally, given that we measure an increase of the cell radius (R_c) of $\leqslant 5\%$ for the hypo-osmotic shock experiments described below, we also make the assumption that this small change does not affect the dynamics of the system appreciably.

We now describe how the thermal fluctuations of a bead, chemically bound to a cell, can be investigated to determine the viscoelastic properties of the cell through the analysis of the time dependence of the bead's mean-square displacement (MSD) $\left\langle \Delta r^2(\tau) \right\rangle \equiv \left\langle [\vec{r}(t+\tau) - \vec{r}(t)]^2 \right\rangle_t$, in the radial direction of the cell; where t is the absolute time and τ is the lag-time (i.e. time interval). The average is taken over all initial times t. Under these circumstances, at thermal equilibrium, it is

Downloaded From: http://proceedings.spiedigitallibrary.org/ on 05/30/2013 Terms of Use: http://spiedl.org/terms

possible to show that Equation 2 can be reorganised to express the viscoelastic moduli of the cell as function of the Fourier transform of the mean-square displacement:

$$\frac{G_c^*(\omega)}{G_0'} = \frac{1}{i\omega\hat{\Pi}(\omega)} + \frac{m\omega^2}{\beta G_0'} - \frac{6\pi R G_s^*(\omega)}{\beta G_0'} \tag{3}$$

where G_0' is the limiting value, for vanishingly low frequencies, of the elastic modulus of the compound system (i.e. cell *plus* solvent), which in this work is $G_0' \equiv G_c^*(\omega)$ for $\omega \to 0$; and $\hat{\Pi}(\omega)$ is the Fourier transform of the normalised mean-square displacement $\Pi(\tau) = 0.5\left\langle \Delta r^2(\tau)\right\rangle / \left\langle r^2\right\rangle$, introduced by Tassieri *et al.*[24] in the study of the thermal fluctuations of an optically trapped bead suspended in a viscoelastic fluid. The term $\left\langle r^2\right\rangle$ is the time-independent variance of $\vec{r}(t)$ from its mean value $\bar{r} \equiv 0$, which we impose to be equal to zero for simplicity. Moreover, it has been shown[24] that for a constrained bead (e.g. optically trapped or, as in this work, chemically bonded to the cell) $\Pi(\tau) = 1$ at large time intervals. In addition, it is important to highlight that, in analogy to an optically trapped bead, the term $\beta G_0'$ can be determined by means of the principle of equipartition of energy, which in one dimension is written as:

$$k_B T = \beta G_0' \langle r^2 \rangle \tag{4}$$

Usefully, two further simplifications can be made to Equation 3 because (*a*) for micron-sized silica beads, the inertia term $m\omega^2$ is negligible up to frequencies on the order of MHz and (*b*) for solvents having frequency-independent viscosity η_s (e.g. water), $G_s^*(\omega)$ simplifies to $i\omega\eta_s$ and the last term in Equation 3 turns to be negligible for the range of frequencies explored in this work. Thus, Equation 3 can be further simplified to:

$$\frac{G_c^*(\omega)}{G_0'} = \frac{1}{i\omega\hat{\Pi}(\omega)}, \tag{5}$$

which provides the viscoelastic properties of the cell (scaled by G_0') over a range of frequencies that is limited at the top end by the acquisition rate of the bead position detector, and at the bottom end by a cutoff frequency given by $\omega_{cutoff} = \beta G_0'/\eta_0$, where η_0 is the limiting value, for vanishing frequencies, of the viscosity of the compound system (i.e. cell *plus* solvent). Notably, Equation 5 is similar to Equation A.6 derived by Tassieri *et al.*[25] to describe the dynamic response of a compound system formed by an optically trapped bead suspended into a generic fluid. Finally, in order to evaluate the Fourier transform in Equation 5 we adopt the analytical method initially introduced by Evans *et al.*[26] (i.e. Eq. (10) of Ref.[26]) and then improved by Tassieri *et al.*[25], which is applied directly to the experimental data points and has the advantage of removing the need for Laplace and inverse-Laplace transformations of experimental data[27].

3. RESULTS AND DISCUSSION

3.1 Bench Test of the method

In order to validate the proposed experimental procedure, we tested it by measuring the linear viscoelastic properties of a soft solid, i.e. cross-linked polydimethylsiloxane (PDMS, Sylgard 184, Dow Corning). In particular, we observed the thermal fluctuations of single beads attached to the exterior of PDMS pillars (having dimensions of $\sim 30\mu m \pm 6\mu m$ in height and $\sim 15\mu m \pm 3\mu m$ in diameter; see inset of Figure 2, right), which were prepared using standard soft lithography techniques. Briefly, PDMS was cast on an Su-8 mold using an elastomer to curing agent ratio of $50:1$ (*w/w*) and thermally cured for $2h$ at $70\ ^oC$. The PDMS structure was irreversibly bonded to a glass coverslip using plasma oxidation ($30s$, $50W$). Figure 2 (left) shows the time evolution of the normalised mean-square displacement of a $5\mu m$ diameter silica bead attached at the top-end of the PDMS pillar, as schematically shown from the inset of the same figure. For simple geometries, like the pillar in this case, the product $\beta G_0'$ is known[28]: i.e. $\beta G_0' = (3\pi E D^4)/(64L^3)$, where E is the Young's modulus, D and L are the diameter and the height of the pillar, respectively.

From Equation 4 it follows that, based on an observed value of the variance of $\left\langle r^2\right\rangle \cong 2x10^{-5}\mu m^2$, we obtain a value of the Young's modulus to be of the order of $E \approx 2kPa$, which is in good agreement with the values shown in literature[29].

Downloaded From: http://proceedings.spiedigitallibrary.org/ on 05/30/2013 Terms of Use: http://spiedl.org/terms

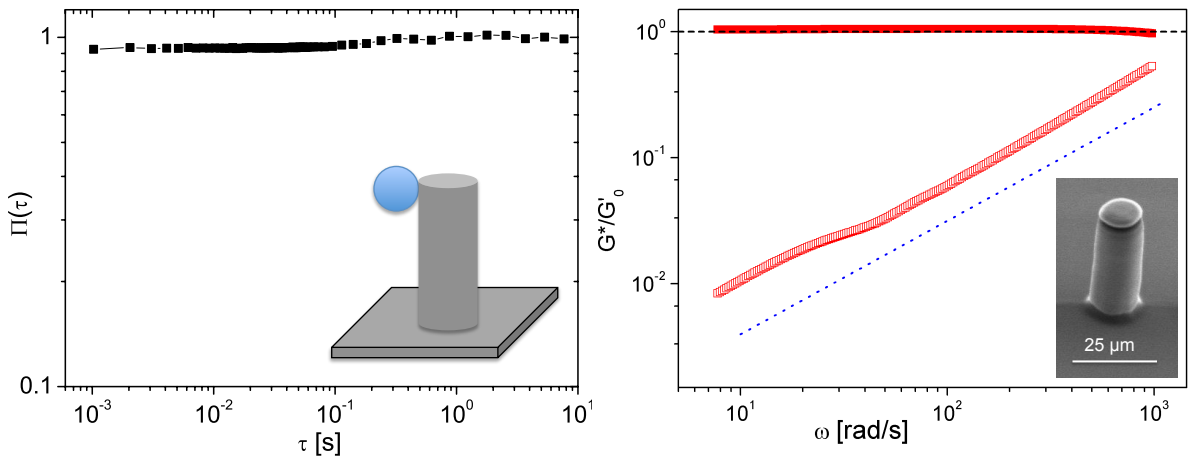

Figure 2. (Left) The normalised mean-square displacement *vs.* lag-time of a 5 μm diameter streptavidin-coated silica bead attached to a PDMS pillar; where $\langle r^2 \rangle \cong 2x10^{-5}\mu m^2$. The inset is a schematic view of the PDMS device. (Right) The normalised complex modulus *vs.* frequency evaluated *via* Equation (5) applied to the data shown in Figure 2. The lines are guides for the gradients. The inset shows a scanning electron microscope image of the PDMS pillar.

Moreover, by applying Equation 5 to the data shown in Figure 2 (left) we obtain the (expected) frequency behaviour of PDMS' viscoelastic moduli; i.e. $G'(\omega) \cong$ constant and $G''(\omega) \ll G'(\omega)$ at low frequencies (see Figure 2, right).

Confident of the validity of our analytical model, we now investigate its applicability to cellular physiology studies by focussing on changes in the cells' microrheology due to either variations in osmolarity of the solution *or* addition of blebbistatin in the cells' bath.

3.2 Cells' response to a hypotonic shock

Osmotic regulation and the transport of osmotically active molecules are fundamental to both metabolic processes and homeostasis of cells and require precise regulation and maintenance of intracellular water[30]. The ability of many cells to regulate their volume, *via* internal restructuring, in response to osmotic changes in their environment is an essential component of normal cellular function. This regulatory volume change is known to be linked to a reorganisation of the cytoskeletal actin networks[31,32]. Exposure to a hypotonic solution typically induces an initial rapid swelling followed by a shrinkage of the cell that occurs over a slower timescale of several minutes. The modulation of the actin dynamics and polymerisation that accompanies these regulatory volume changes has been shown in various cell types by methods such as DNase I inhibition assay and fluorescence measurements of phalloidin-labelled actin[31].

It is anticipated that there are two major physiological processes that accompany the changes in osmolarity of the solution surrounding the Jurkat cell: (I) an actin cytoskeleton reorganisation and (II) an increase of the cell volume as the solution becomes hypo-osmotic. In order to quantify the changes in cell volume, we assumed that the cells were spherical, Figure 1. In particular, Figure 3 shows that the relative radius changes are $< 6\%$ when the surrounding media was made hypo-osmotic by addition of 10% v/v distilled water. The data of Figure 3 also shows that, after an initial swelling, the cells contract to a still swollen state that is $\sim$5% larger than when they were in isotonic media. Based on these observations, which are in close agreement with those already existing in literature[33], we assume that these small radius changes do not affect the dynamics of the system appreciably, as discussed in the next section.

To study how the *in vivo* viscoelastic properties of Jurkat cells vary with the osmolarity of the solution, we have adopted the model described earlier. In particular, analysis of different time regimes in the time dependent normalised mean-squared displacement, $\Pi(\tau)$, has the potential to reveal information both on the pure elastic component of the cell (at long time intervals or low frequencies) and on the fast dynamics occurring at small length scales (e.g. those related to the transverse bending modes of single actin filaments in the cytoskeleton).

Downloaded From: http://proceedings.spiedigitallibrary.org/ on 05/30/2013 Terms of Use: http://spiedl.org/terms

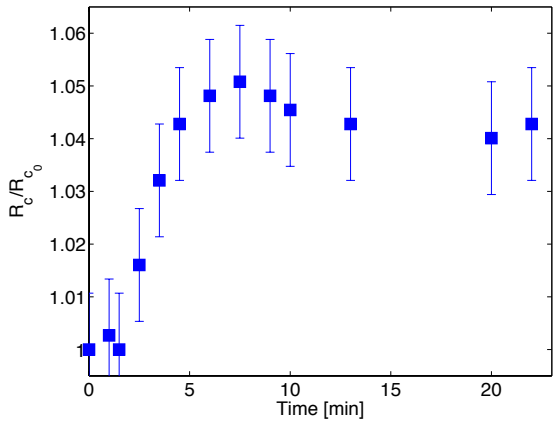

Figure 3. Averaged relative cell radius changes *vs.* time as a consequence of the change in osmolarity of the cell solution; from iso-osmotic conditions in PBS buffer towards a hypo-osmotic condition obtained by adding 10% v/v of distilled water to the initial solution. The osmotic shock causes a rapid swelling of the cells, followed by a partial recovery of the cells' volume. These results are in good agreement with those reported in literature[33].

3.2.1 Elastic properties of the cell derived from $\Pi(\tau)$

The first result that can be obtained through the analysis of the thermal fluctuations of the bound bead (Figure 1) is the relative change of the cell's low frequency elastic plateau modulus $G_c'(0)$, Figure 4. This can be evaluated from the time-independent variance $\langle r^2 \rangle$ of the constrained bead in the radial direction of the cell, by adopting the principle of equipartition of energy as in Equation 4. In particular, although the absolute value of $G_c'(0)$ can not be determined because of the unknown factor β, the relative change between different values of $\beta G_c'(0)$, obtained from n sequential measurements performed on the same cell, differ from each other only because of both the small increase of the cell radius (measured as $\sim$5%) and the variation of $G_c'(0)$. Thus, from Figure 4 it is clear that a change of 10% in osmolarity towards hypotonicity, which occurs at t $\sim$9min as a result of adding distilled water to the iso-osmotic solution, induces a temporary increase of $\beta G_c'(0)$ that lasts for approximately 15-30min. At its greatest, this change in the low frequency elastic modulus dependent term, $\beta G_c'(0)$, is over 3 fold in magnitude.

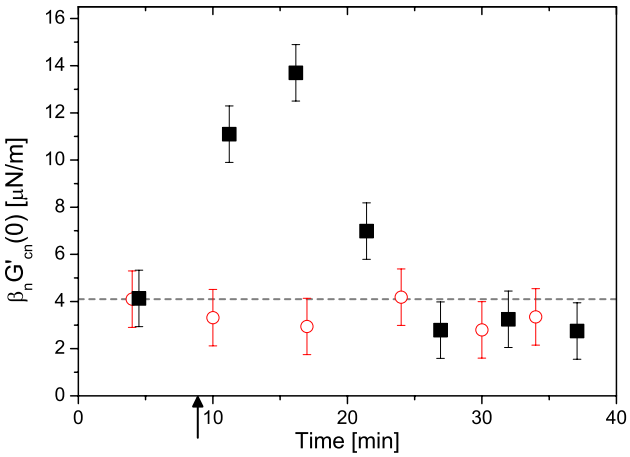

Figure 4. The absolute value of $\beta G_c'(0)$ measured in isotonic (PBS) condition (circle symbols) and when the solution is made 10% hypotonic (square symbols). The arrow indicates the time at which the isotonic solution is made hypotonic. The dotted line is a guide for the eye, so that the later points in the graph can be compared to the first points measured in isotonic condition.

Downloaded From: http://proceedings.spiedigitallibrary.org/ on 05/30/2013 Terms of Use: http://spiedl.org/terms

The explanation for such a large increase may in part be due to the change in radius; however, if this were solely responsible, it would be expected that $\beta G_c'(0)$ would remain significantly above its original value, as the cells do not regain their original radius (as shown in Figure 3). Thus, since $\beta G_c'(0)$ *does* return to close to the original value (at $t \sim$25 min), consideration should be given to the temporary increase in electrostatic intermolecular interactions within the cell due to the reduction in ionic strength of the solution (i.e. a reduction in screening of the charges on cytoskeleton molecules by solution based ions). This latter phenomenon would also alter the cell's viscoelastic properties and any resulting actin cytoskeleton rearrangement may be seen as part of an attempt of the cell to re-equilibrate the solution osmolarity, as discussed below.

3.2.2 Fast dynamics of the cell derived from $\Pi(\tau)$

In order to study the high frequency behaviour of cells, we have used Equation 5, which directly relates the normalised mean-square displacement, $\Pi(\tau)$, of the bead to the cell complex modulus, $G_c^*(\omega)$. In particular, we have applied Equation 5 to the $\Pi(\tau)$ derived from measurements that were collected at fixed time intervals after the solution was made hypotonic. In Figure 5, these are compared with the normalised MSD of the same cell in phosphate-buffered saline (PBS) solution, prior to hypotonic exposure. Note that in order to more easily discern visually the changes in $\Pi(\tau)$, caused by the hypotonicity, the normalised MSD for the cell in PBS is plotted in each of the panels.

The elastic ($G_c'(\omega)$) and viscous ($G_c''(\omega)$) components of the complex modulus, $G_c^*(\omega)$, derived from the measurements shown in Figure 5 are shown in Figure 6 (scaled by the plateau modulus $G_c'(0)$). It is clear that, in PBS (Figure 6A), the high frequency behaviour of the cell's elastic and viscous moduli both show a frequency dependence of $\propto \omega^{3/4}$, which is characteristic of isotropic *in vitro* reconstituted actin filament solutions[34,35]. As the solution is made hypo-osmotic, the cell cytoskeleton starts to reorganise and the frequency behaviour of the moduli drastically change as (sequentially) shown in Figure 6. In particular, after $\sim$10min in the hypo-osmotic solution both moduli tend to assume a high frequency behaviour $\propto \omega^{1/2}$ (see Figures 6C). This change in the degree of elasticity may be explained by an increase in cytoskeletal tension as response to a stretching force caused by the cell swelling.

Finally, it is important to highlight that the results that have been obtained here using a video particle tracking method are in good agreement with those presented in the review written by Papakonstanti and Stournaras[31], where a set of assessments of actin cytoskeleton dynamics and actin architecture in cell volume regulation are summarised. However, none of the techniques reviewed in that work[31] are able to provide quantitative information on the cell viscoelasticity, as is the case here.

Downloaded From: http://proceedings.spiedigitallibrary.org/ on 05/30/2013 Terms of Use: http://spiedl.org/terms

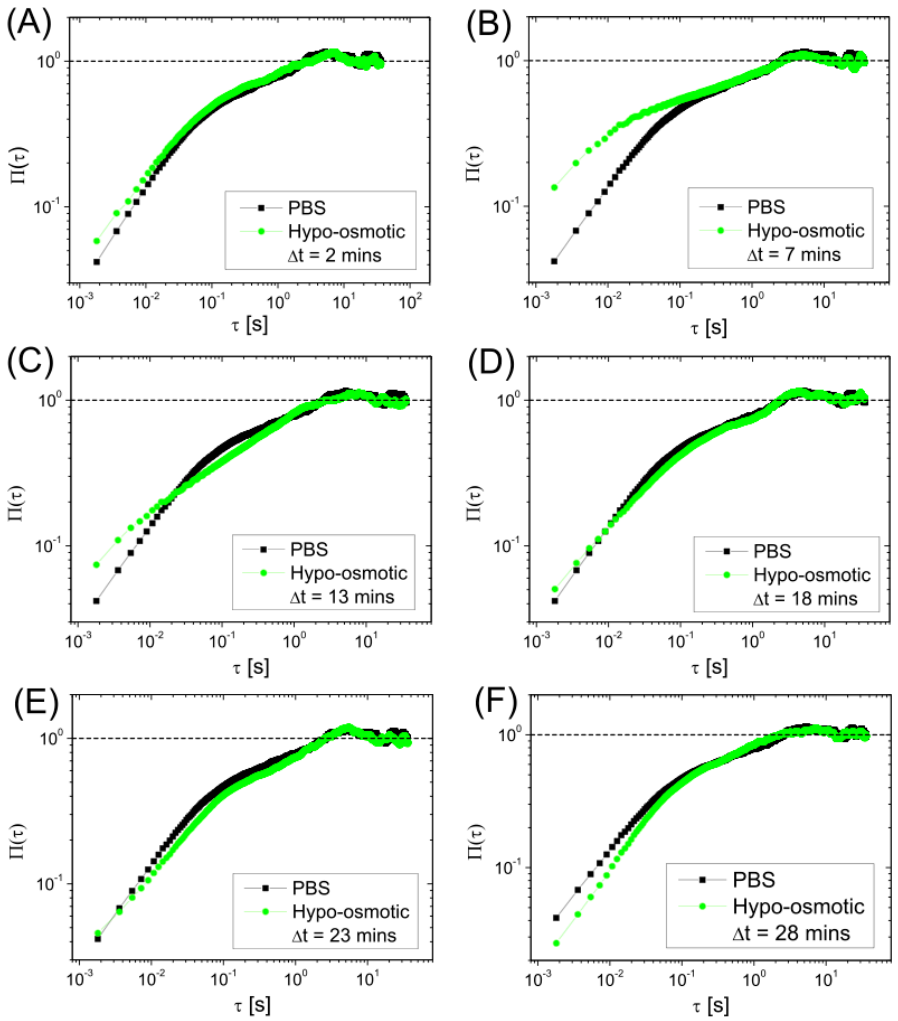

Figure 5. The normalised mean-square displacement *vs.* lag-time of a 5 μm diameter silica bead chemically bound to a Jurkat cell in iso-osmotic (PBS) solution (square symbols) and in hypo-osmotic solution (circle symbols) after the addition of 10% v/v distilled water to the PBS buffer and measured at time intervals (Δt) of (A) 2 min, (B) 7 min, (C) 12 min, (D) 18 min, (E) 23 min, (F) 28 min, respectively. At short time intervals, the $\Pi(\tau)$ has the potential to reveal the dynamics occurring at molecular level (as shown in Figure 6); whereas, at large lag-times it provides information on the stiffness of the whole cell (as shown in Figure 4).

Downloaded From: http://proceedings.spiedigitallibrary.org/ on 05/30/2013 Terms of Use: http://spiedl.org/terms

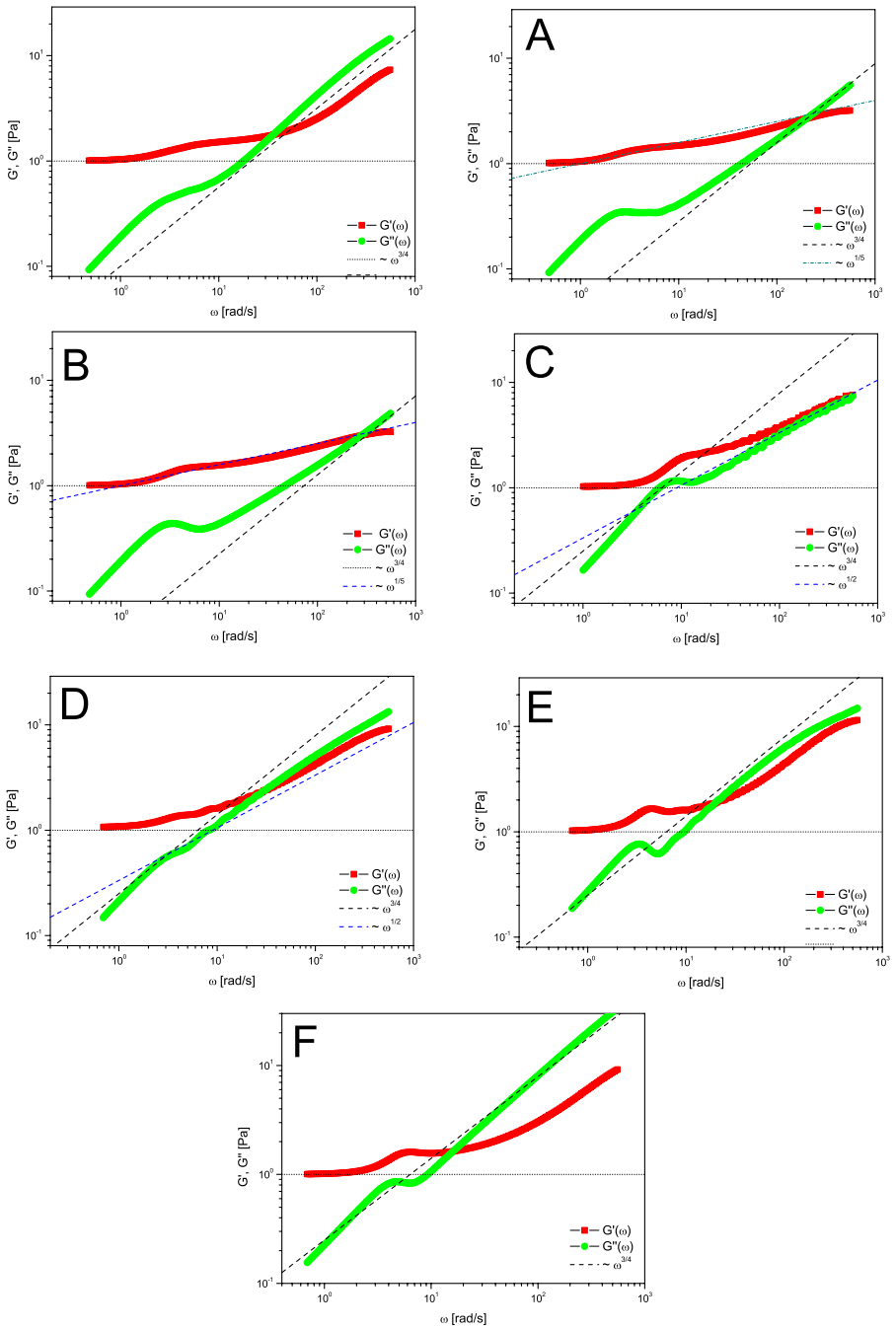

Figure 6. The real (storage, $G_c'(\omega)$) and the imaginary (loss, $G_c''(\omega)$) parts of the complex modulus ($G_c^*(\omega)$) scaled by G_0' *vs.* frequency of a Jurkat cell in iso-osmotic (PBS) solution (top-left) and in hypo-osmotic solution (A-F) after the addition of 10% v/v distilled water to the PBS buffer and measured at time intervals (Δt) of (A) 2 min, (B) 7 min, (C) 12 min, (D) 18 min, (E) 23 min, (F) 28 min, respectively. The moduli have been evaluated by using Equation 5 on the normalised mean-square displacement data shown in Figure 5. The lines are guides for the gradients.

Downloaded From: http://proceedings.spiedigitallibrary.org/ on 05/30/2013 Terms of Use: http://spiedl.org/terms

3.3 Cells' response to blebbistatin

Non-muscle myosin-II is an actin-binding protein that has actin cross-linking and contractile properties and is regulated by the phosphorylation of its light and heavy chains. It is central in the control of cell adhesion, cell migration and tissue architecture[36]. Blebbistatin is a small molecule that demonstrates high affinity and specificity towards myosin-II by binding to the ADP/phosphate complex at the active site, which inhibits the release of the phosphate and prevents myosin from entering into the cross-bridge cycle with actin[37]. This does not interfere with the binding of myosin to actin, but instead blocks the myosin heads in a products complex with low actin affinity[37]. Moreover, from a rheological point of view, it is yet to be resolved how transiently cross-linking proteins affect the frequency response of cross-linked actin networks in the elasticity dominated intermediate frequency regime. It has been shown[8], during *in vitro* studies, that transiently cross-linking proteins can be characterised by an off rate k_{off} that typically corresponds to frequencies in the intermediate regime of several *mHz* up to a few *Hz*.

To study how the *in vivo* viscoelastic properties of Jurkat cells vary with the addition of blebbistatin to the cells' bath, we have proceeded in the same way as described for the case where the solution osmolarity was changed. In particular, we have monitored the cells' response to the addition of $25\mu M$ of blebbistatin by measuring the thermal fluctuations of a bead chemically bound to the cell's exterior (Figure 1) and analysed the different time regimes *via* the time-dependent normalised mean-squared displacement, $\Pi(\tau)$; which has the potential of revealing the cells' viscoelastic properties by means of Equation 5.

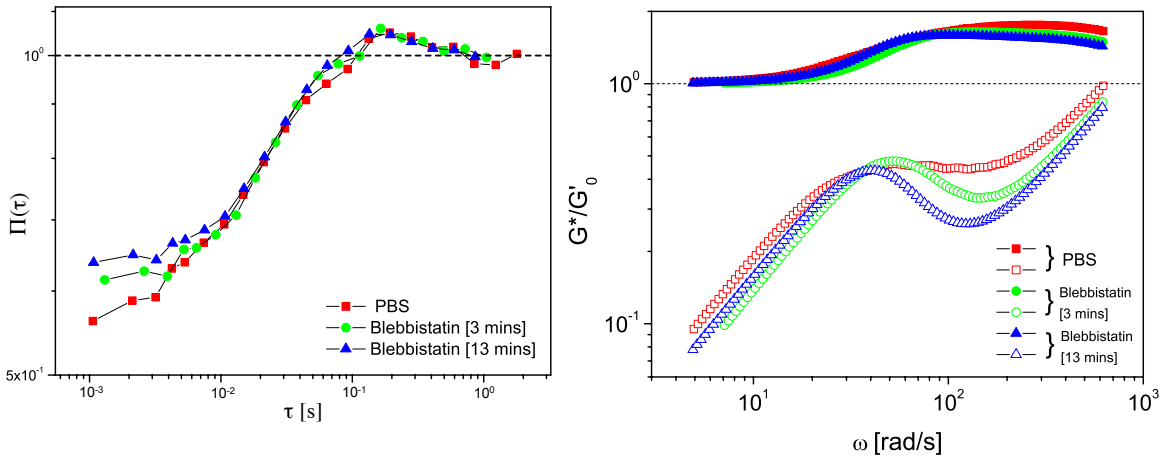

Figure 7. (Left) The normalised mean-square displacement *vs.* lag-time of a 5 μm diameter silica bead chemically bound to a Jurkat cell in PBS (red symbols) and and after the addition of $1\mu M$ of blebbistatin to the cells' bath and measured at time intervals 3 min (green symbols) and 13 min (blue symbols), respectively. (Right) The storage ($G'_c(\omega)$, filled symbols) and the loss ($G''_c(\omega)$, open symbols) moduli scaled by G'_0 *vs.* frequency of a Jurkat cell in PBS (red symbols) and after the addition of blebbistatin to the cells' bath and measured at time intervals 3 min (green symbols) and 13 min (blue symbols), respectively. The moduli have been evaluated by using Equation 5 on the normalised mean-square displacement data shown on the left.

3.3.1 Low frequency response of the cell derived from $\Pi(\tau)$

In contrast with the results presented here for the case of the hypotonic shock, where the cell's low frequency elastic plateau modulus $G'_c(0)$ was changing by over 3 fold in magnitude, we report that the addition of $1\mu M$ of blebbistatin to the cells' bath does not change substantially the value of $G'_c(0)$. This result is in good agreement with those present in literature[9].

3.3.2 Fast dynamics of the cell derived from $\Pi(\tau)$

Figure 7 show a typical result obtained from the analysis of measurements performed on a single cell when blebbistatin is added to the cell's bath. In particular, in Figure 7 (left) are compared the normalised MSDs measured on a single cell

Downloaded From: http://proceedings.spiedigitallibrary.org/ on 05/30/2013 Terms of Use: http://spiedl.org/terms

initially in phosphate-buffered saline (PBS) solution and after the addition of $1\mu M$ of blebbistatin. The high frequency response of the cell (see Figure 7, right) is evaluated via Equation 5, which relates $\Pi(\tau)$ to the cell's complex modulus, $G_c^*(\omega)$. However, although the absolute value of the cells' complex modulus is not yet achievable, the frequency behaviour of the moduli can provide useful information, too. Indeed, when the results shown in Figure 7 (right) are compared with those obtained from *in vitro* reconstituted actin–myosin-II networks[8], the agreement between the frequency behaviour of both the moduli is good. Moreover, by fitting the data shown in Figure 7 (right) with the model suggested by Lieleg *et al.*[8], we obtain a value of k_{off} of two order of magnitude higher than the *in vitro* case; this is consistent with the fact that in our experiments we actually add $1\mu M$ of blebbistatin, which enhances the off rate.

Conclusions

In summary, we have presented a straightforward and *non-invasive* experimental procedure, coupled with a new analytical method to interpret the data, which leads to quantitative determination of the *in vivo* viscoelastic properties of cells in the frequency domain. The method has the potential to monitor the internal dynamics and re-organisation of the actin cytoskeleton up to frequencies on the order of kHz, representing a valuable addition to studies that address cellular physiology and pharmacological response. Indeed, in this work we report, *for the first time*, the high frequencies (up to $\sim 1kHz$) changes of the Jurkat cells' viscoelastic spectrum from $\propto \omega^{3/4}$ to $\propto \omega^{1/2}$, as response to a change in osmolarity of the solution. The rheological interpretation of the results gives a direct insight of the cell cytoskeleton structure and its re-organisation. In the future, it is envisaged that these interpretations could be coupled with advanced molecular biology techniques to resolve the detailed interactions underlying these rheological changes and that faster dynamics could be studied by means of a quadrant photo-diode based tracking system

Acknowledgments

MT acknowledges support via personal research fellowship from the Royal Academy of Engineering/EPSRC. We are grateful to EPSRC and BBSRC for supporting this work through grants EP/F040857/1 and BB/C511572/1, respectively, and to the DTC in Proteomic and Cell Technologies (EPSRC) for funding RLW. The funders had no role in study design, data collection and analysis, decision to publish, or preparation of the manuscript.

References

[1] Jordan, P., Leach, J., Padgett, M., Blackburn, P., Isaacs, N., Goksor, M., Hanstorp, D., Wright, A., Girkin, J., and Cooper, J., "Creating permanent 3d arrangements of isolated cells using holographic optical tweezers," *Lab Chip* **5**, 1224–1228 (2005).

[2] Watts, F., Tan, L. E., Tassieri, M., McAlinden, N., Wilson, C. G., Girkin, J. M., and Wright, A. J., "The viscoelastic properties of the vitreous humor measured using an optically trapped local probe.," *Proceedings of SPIE* **8097**, SPIE (2011).

[3] Tassieri, M., Evans, R., Barbu-Tudoran, L., Trinick, J., and Waigh, T., "The self-assembly, elasticity, and dynamics of cardiac thin filaments," *Biophysical Journal* **94**, 2170–2178 (2008).

[4] Bertseva, E., Grebenkov, D., Schmidhauser, P., Gribkova, S., Jeney, S., and Forro, L., "Optical trapping microrheology in cultured human cells," *European Physical Journal E* **35** (JUL 2012).

[5] Chicurel, M., Chen, C., and Ingber, D., "Cellular control lies in the balance of forces," *Current Opinion in Cell Biology* **10**, 232–239 (APR 1998).

[6] Lau, A. W., Hoffman, B. D., Davies, A., Crocker, J. C., and Lubensky, T. C., "Microrheology, stress fluctuations, and active behavior of living cells," *Phys Rev Lett* **91**, 198101–198101 (Nov 2003).

Downloaded From: http://proceedings.spiedigitallibrary.org/ on 05/30/2013 Terms of Use: http://spiedl.org/terms

[7] Mizuno, D., Tardin, C., Schmidt, C. F., and Mackintosh, F. C., "Nonequilibrium mechanics of active cytoskeletal networks," *Science* **315**, 370–373 (Jan 2007).

[8] Lieleg, O., Claessens, M. M., Luan, Y., and Bausch, A. R., "Transient binding and dissipation in cross-linked actin networks," *Phys Rev Lett* **101**, 108101–108101 (Sep 2008).

[9] Hale, C. M., Sun, S. X., and Wirtz, D., "Resolving the role of actoymyosin contractility in cell microrheology," *PLoS One* **4**(9), e7054 (2009).

[10] Kollmannsberger, P. and Fabry, B., "Linear and Nonlinear Rheology of Living Cells," *Annual Review of Materials Research* **41**, 75–97 (2011).

[11] Wolff, L., Fernandez, P., and Kroy, K., "Resolving the Stiffening-Softening Paradox in Cell Mechanics," *PLOS ONE* **7** (JUL 16 2012).

[12] Ferry, J. D., [*Viscoelastic properties of polymers*], Wiley, 3d ed ed. (1980).

[13] Bausch, A., Ziemann, F., Boulbitch, A., Jacobson, K., and Sackmann, E., "Local measurements of viscoelastic parameters of adherent cell surfaces by magnetic bead microrheometry," *Biophysical Journal* **75**, 2038–2049 (Oct. 1998).

[14] Bausch, A., Hellerer, U., Essler, M., Aepfelbacher, M., and Sackmann, E., "Rapid stiffening of integrin receptor-actin linkages in endothelial cells stimulated with thrombin: A magnetic bead microrheology study," *Biophysical Journal* **80**, 2649–2657 (June 2001).

[15] Deng, L., Trepat, X., Butler, J. P., Millet, E., Morgan, K. G., Weitz, D. A., and Fredberg, J. J., "Fast and slow dynamics of the cytoskeleton," *Nature Materials* **5**, 636–640 (Aug. 2006).

[16] Hoh, J. H. and Schoenenberger, C. A., "Surface morphology and mechanical properties of mdck monolayers by atomic force microscopy," *J Cell Sci* **107 (Pt 5)**, 1105–14 (May 1994).

[17] Uhde, J., Feneberg, W., Ter-Oganessian, N., Sackmann, E., and Boulbitch, A., "Osmotic force-controlled microrheometry of entangled actin networks," *Phys Rev Lett* **94**, 198102 (May 2005).

[18] Wirtz, D., "Particle-tracking microrheology of living cells: principles and applications," *Annu Rev Biophys* **38**, 301–26 (2009).

[19] Lu, Y.-B., Franze, K., Seifert, G., Steinhäuser, C., Kirchhoff, F., Wolburg, H., Guck, J., Janmey, P., Wei, E.-Q., Käs, J., and Reichenbach, A., "Viscoelastic properties of individual glial cells and neurons in the cns," *Proc Natl Acad Sci U S A* **103**, 17759–64 (Nov 2006).

[20] Rogers, S. S., Waigh, T. A., and Lu, J. R., "Intracellular microrheology of motile amoeba proteus," *Biophysical Journal* **94**, 3313–3322 (Apr. 2008).

[21] Gibson, G. M., Leach, J., Keen, S., Wright, A. J., and Padgett, M. J., "Measuring the accuracy of particle position and force in optical tweezers using high-speed video microscopy," *Opt Express* **16**, 14561–70 (Sep 2008).

[22] Kulin, S., Kishore, R., Hubbard, J. B., and Helmerson, K., "Real-time measurement of spontaneous antigen-antibody dissociation," *Biophys J* **83**, 1965–73 (Oct 2002).

[23] Mason and Weitz, "Optical measurements of frequency-dependent linear viscoelastic moduli of complex fluids," *Phys Rev Lett* **74**, 1250–1253 (Feb 1995).

[24] Tassieri, M., Gibson, G. M., Evans, R. M. L., Yao, A. M., Warren, R., Padgett, M. J., and Cooper, J. M., "Measuring storage and loss moduli using optical tweezers: Broadband microrheology," *Physical Review E* **81**, 026308 (Feb. 2010).

[25] Tassieri, M., Evans, R. M. L., Warren, R. L., Bailey, N. J., and Cooper, J. M., "Microrheology with optical tweezers: data analysis," *New Journal of Physics* **14**(11), 115032 (2012).

Downloaded From: http://proceedings.spiedigitallibrary.org/ on 05/30/2013 Terms of Use: http://spiedl.org/terms

[26] Evans, R. M. L., Tassieri, M., Auhl, D., and Waigh, T. A., "Direct conversion of rheological compliance measurements into storage and loss moduli," *Phys Rev E* **80**, 012501 (Jul 2009).

[27] Mason, T., Ganesan, K., vanZanten, J., Wirtz, D., and Kuo, S., "Particle tracking microrheology of complex fluids," *Physical Review Letters* **79**, 3282–3285 (Oct. 1997).

[28] Gere, J. M., "Mechanics of materials. 5th," *Brooks Cole* (2001).

[29] Ochsner, M., Dusseiller, M. R., Grandin, H. M., Luna-Morris, S., Textor, M., Vogel, V., and Smith, M. L., "Micro-well arrays for 3d shape control and high resolution analysis of single cells," *Lab Chip* **7**, 1074–1077 (2007).

[30] Nagy, T., Balasa, A., Frank, D., Rab, A., Rideg, O., Kotek, G., Magyarlaki, T., Bogner, P., Kovács, G. L., and Miseta, A., "O-glcnac modification of proteins affects volume regulation in jurkat cells," *Eur Biophys J* **39**, 1207–17 (Jul 2010).

[31] Papakonstanti, E. A. and Stournaras, C., "Actin cytoskeleton architecture and signaling in osmosensing," *Methods Enzymol* **428**, 227–40 (2007).

[32] Ebner, H. L., Cordas, A., Pafundo, D. E., Schwarzbaum, P. J., Pelster, B., and Krumschnabel, G., "Importance of cytoskeletal elements in volume regulatory responses of trout hepatocytes," *Am J Physiol Regul Integr Comp Physiol* **289**, R877–90 (Sep 2005).

[33] Cantiello, H., "Role of actin filament organization in cell volume and ion channel regulation," *Journal of Experimental Zoology* **279**, 425–435 (Dec. 1997).

[34] Farge, E. and Maggs, A., "Dynamic scattering from semiflexible polymer," *Macromolecules* **26**, 5041–5044 (Sept. 1993).

[35] Tassieri, M., Evans, R. M. L., Barbu-Tudoran, L., Khaname, G. N., Trinick, J., and Waigh, T. A., "Dynamics of semiflexible polymer solutions in the highly entangled regime," *Physical Review Letters* **101**, 198301 (Nov. 2008).

[36] Vicente-Manzanares, M., Ma, X., Adelstein, R. S., and Horwitz, A. R., "Non-muscle myosin II takes centre stage in cell adhesion and migration," *Nature Reviews Molecular Cell Biology* **10**, 778–790 (NOV 2009).

[37] Kovács, M., Tóth, J., Hetényi, C., Málnási-Csizmadia, A., and Sellers, J., "Mechanism of blebbistatin inhibition of myosin ii.," *The Journal of biological chemistry* **279**(34), 35557–35563 (2004).

Downloaded From: http://proceedings.spiedigitallibrary.org/ on 05/30/2013 Terms of Use: http://spiedl.org/terms